Supporting information

# Geometrical engineering of SPAN-graphene composite cathode for practical Li-S batteries

Hun Kim,[a,‡] Jang-Yeon Hwang,[b,‡] Sangin Bang,[a,‡] Hun-Gi Jung,[c] and Yang-Kook Sun[*,a]

[a.] Department of Energy Engineering, Hanyang University, Seoul 04763, Republic of Korea.

[b.] Department of Materials Science and Engineering, Chonnam National University, Gwangju 61186, Republic of Korea.

[c.] Center for Energy Storage Research, Korea Institute of Science and Technology, Seoul 02792, Republic of Korea.

‡ These authors contributed equally to this work.

*Correspondence author: yksun@hanyang.ac.kr

**Table S1.** Elemental analysis of SPAN.

| Sample | Sulfur (wt%) | Carbon (wt%) | Nitrogen (wt%) | Hydrogen (wt%) |
|---|---|---|---|---|
| SPAN | 46.48 | 38.90 | 13.74 | 0.88 |

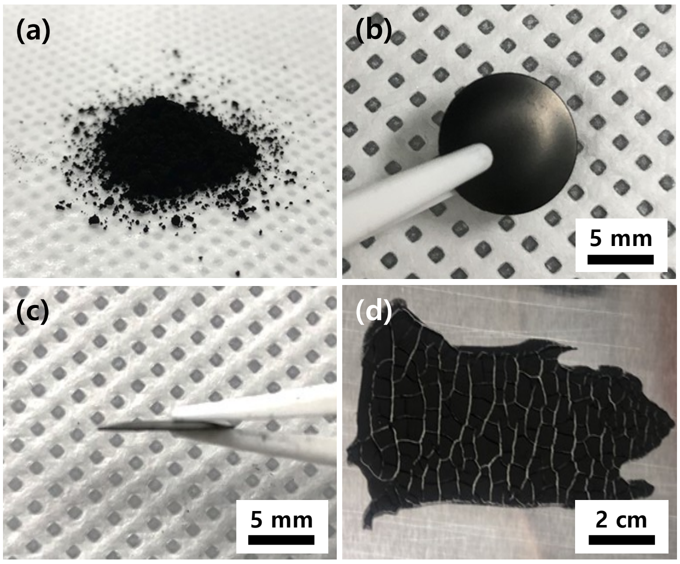


**Fig. S1.** Photographs of (a) a ball-milled SPAN/G mixture, a pelletized 2D-SPAN/G cathode ((b) top-view, (c) side view), and (d) a SPAN/G cathode with a sulfur loading of 5 mg $cm^{-2}$, prepared using a conventional casting method (cracked).

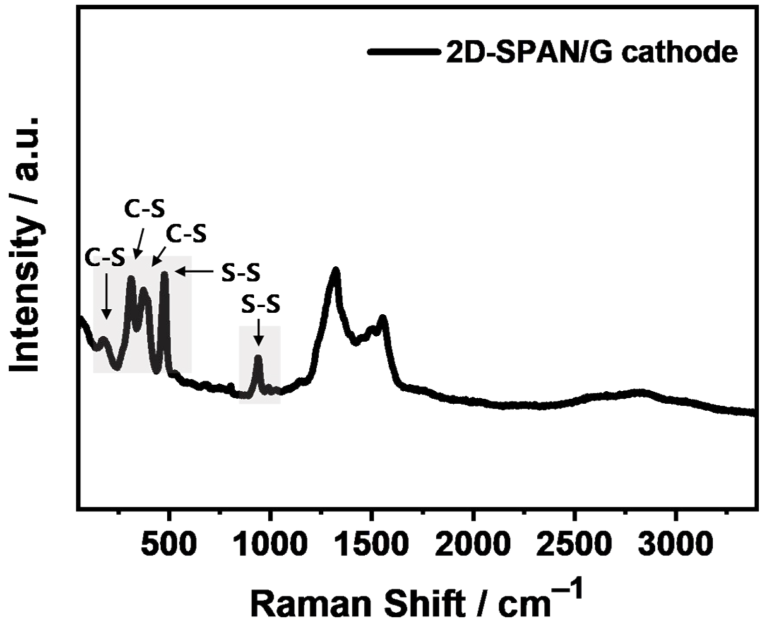


**Fig. S2.** Raman spectra of 2D-SPAN/G cathode.

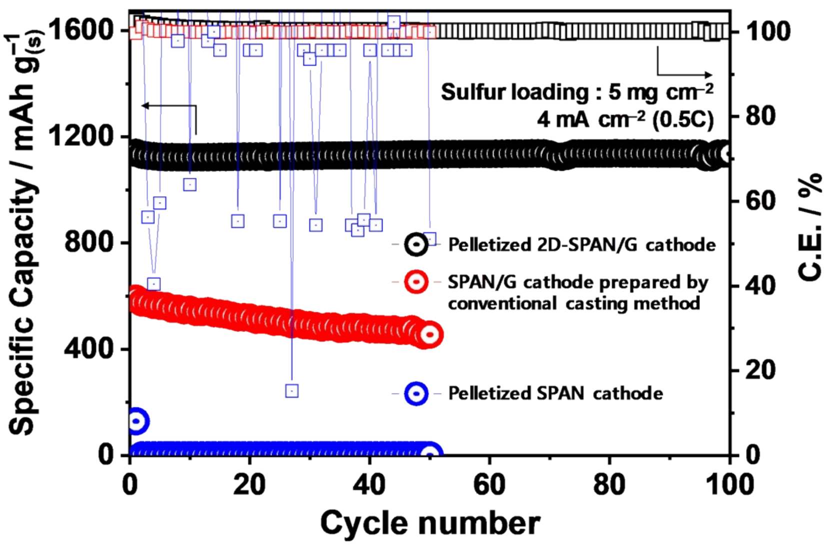


**Fig. S3.** Electrochemical performances of Li-S batteries. Cycling stability of Li-S batteries featuring SPAN/G cathodes prepared by pelletizing method and conventional casting method, and SPAN cathode prepared by pelletizing method with sulfur loadings of 5 mg cm$^{-2}$ (at 4 mA cm$^{-2}$ (0.5C)). Cycling data of the pelletized SPAN/G cathode is reproduced from the Fig. 3c to compare the electrochemical performance of each cathode.

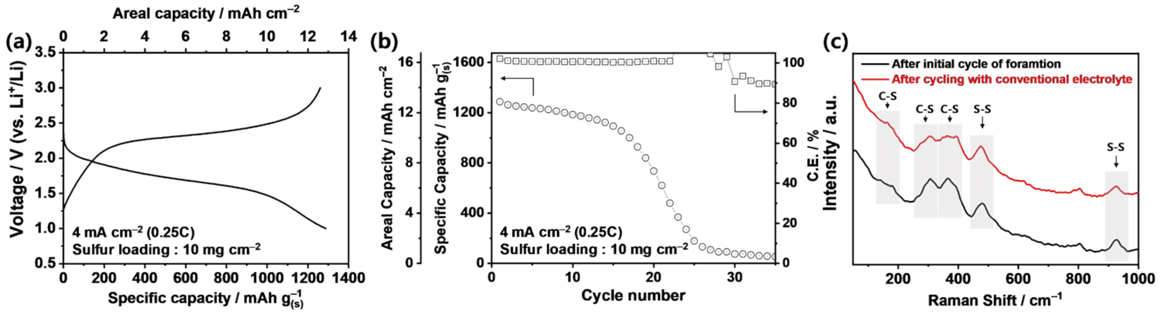


**Fig. S4.** Electrochemical performances of Li–S batteries featuring 2D-SPAN/G cathodes and conventional electrolyte (1 M $LiPF_6$ in EC:EMC (3:7 (v/v))). (a) Charge–discharge profiles of batteries cycled at 4 mA cm$^{-2}$. (b) Cycling stability of a Li–S battery featuring a 2D-SPAN/G cathode with a sulfur loading of 10 mg cm$^{-2}$. (c) Ex-situ Raman spectra of 2D-SPAN/G cathodes recovered from batteries after one cycle and cell failure.

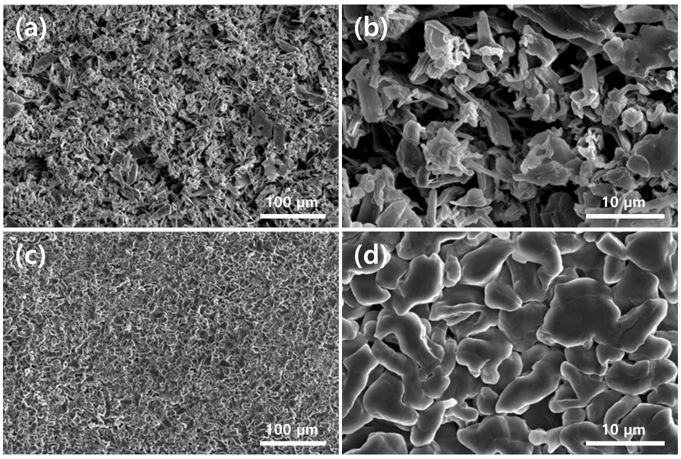


**Fig. S5.** SEM images of Li deposited on Cu foils in (a, b) conventional electrolyte (1 M $LiPF_6$ in EC:EMC (3:7 (v/v))) and (c, d) modified electrolyte (1 M $LiPF_6$ and 0.05 M LiDFOB in EMC:FEC (3:1 (v/v))). Li (capacity of 10 mAh $cm^{-2}$) was deposited on the Cu foils in Li ‖ Cu cells for 10 h.

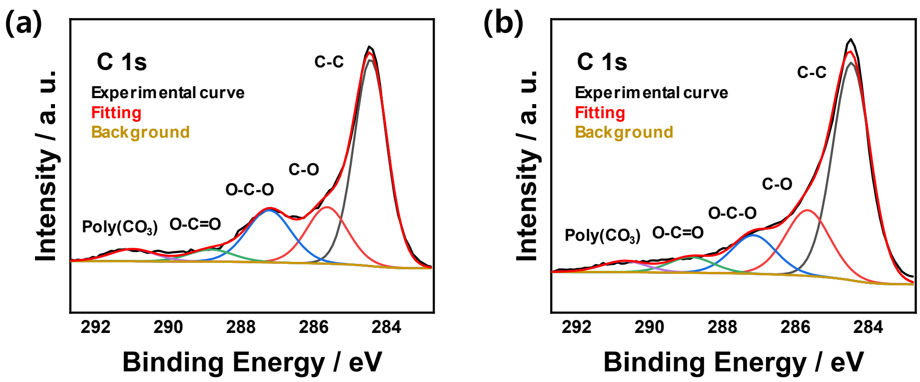


**Fig. S6.** Characterization of cathode/electrode interphase after the 1st cycle. XPS spectra of C 1s for the 2D-SPAN/G cathode operated in (a) conventional electrolyte and (b) modified electrolyte.

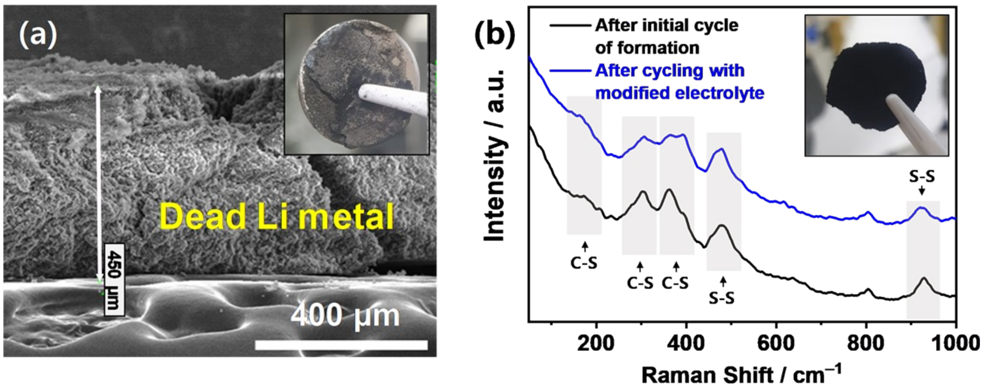


**Fig. S7.** (a) Cross-sectional SEM image of a Li-metal anode subjected to 500 cycles in a Li–S battery; inset: digital photograph of retrieved Li-metal anode. (b) Ex-situ Raman spectra of a 2D-SPAN/G cathode cycled in modified electrolyte after one and 500 cycles; inset: digital photograph of retrieved 2D-SPAN/G cathode.

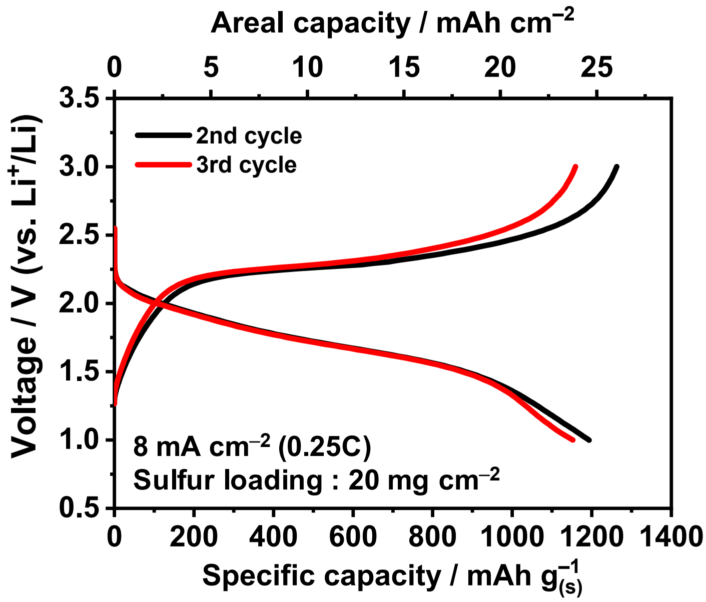


**Fig. S8.** Charge–discharge profiles of a Li–S battery featuring a 2D-SPAN/G cathode with a sulfur loading of 20 mg $cm^{-2}$.

**Table S2.** Summary of reported SPAN-based Li–S batteries and their performances. The power density is calculated based on the cathode (in the case of sulfur loading > 3 mg cm$^{-2}$) and nominal voltage is assumed as 1.8V.

| No. | Strategy | S loading (mg cm$^{-2}$) | Areal capacity (mAh cm$^{-2}$) | Current density (mA cm$^{-2}$) | Power density (W kg$^{-1}$) | Cycle life (cycles) | Retention (%) | Ref. |
|---|---|---|---|---|---|---|---|---|
| 1 | Carboxymethyl cellulose binder | 0.22 | 0.23 | 0.33 | – | 500 | 110.0 | 45 |
| 2 | SPAN-porous carbon | 0.4 | 0.6 | 0.067 | – | 100 | 83.4 | 57 |
| 3 | FEC solvent | 0.5 – 0.7 | 0.9 | 0.28 | – | 1,100 | 89.0 | 71a |
| 4 | Tortuosity SPAN-4 | 0.5 | 0.45 | 0.42 | – | 200 | 95.0 | 71b |
| 5 | Textile Fiber-based S-PAN | 0.67 | 1.0 | 0.5 | – | 1,000 | 77.3 | 71c |
| 6 | LiBOB additive | 0.7 | 1.2 | 0.3 | – | 100 | 62.0 | 71d |
| 7 | SPAN film with hollow tubular nanofiber(H-SPAN film) | 0.7 | 0.88 | 0.12 | – | 300 | 99.0 | 71e |
| 8 | SPAN-SE | 0.86 | 1.2 | 0.17 | – | 200 | 85.0 | 56 |
| 9 | S@pPAN-5 | 0.86 | 1.33 | 0.49 | – | 100 | 88.0 | 71f |
| 10 | $Li_2SiO_3$ additive | 0.93 | 0.9 | 0.08 | – | 100 | 79.0 | 71g |
| 11 | SPAN fiber in Mesoporous carbon polyhedron | 1.0 | 1.5 | 0.16 | – | 200 | 84.4 | 71h |
| 12 | FeS incorporated S-PAN | 1.0 – 1.2 | 1.2 | 6.0 | – | 100 | 72.0 | 71i |
| 13 | Nonflammable electrolyte 1M LiBOB/TEP+FEC (7:3, v/v) | 1.0 | 1.38 | 1.68 | – | 1,000 | 79.0 | 71j |
| 14 | 1wt% TSMP + 2wt% VC additive | 1.0 | 1.47 | 1.68 | – | 800 | 85.0 | 71k |
| 15 | Mesoporous S-PAN | 1.1 | 1.3 | 3.0 | – | 900 | 85.7 | 32 |
| 16 | $NiS_2$ modified S-PAN | 1.15 | 2.0 | 0.23 | – | 100 | 89.0 | 31 |
| 17 | S/DPAN/KB | 1.5 | 1.69 | 0.39 | – | 150 | 81.0 | 46 |
| 18 | SPAN/CNT-12 | 2.0 | 2.36 | 1.59 | – | 800 | 100 | 39 |
| 19 | SPAN/RGO by ball milling | 2.1 – 2.8 | 3.88 | 0.47 | – | 200 | 80.0 | 37 |
| 20 | Iodine doped S-PAN | 2.3 | 2.91 | 7.71 | – | 1,000 | 85.0 | 71l |
| 21 | FEC additive | 2.5 | 4.0 | 0.5 | – | 100 | 98.4 | 64 |
| 22 | Freestanding S/PAN/GO cathode | 2.5 | 3.45 | 0.58 | – | 100 | 87.0 | 71m |
| 23 | Mixing method | 3.0 | 4.0 | 1.0 | – | 80 | 74.0 | 71n |
| 24 | PAA binder + FEC additive | 3.0 | 4.6 | 2.5 | – | 100 | 98.5 | 60 |
| 25 | Te-doped S@pPAN | 3.1 | 3.39 | 0.62 | 120.0 | 100 | 80.0 | 71o |
| 26 | $CoS_2$-SPAN-CNT | 4.6 | 5.06 | 1.81 | 305.9 | 50 | 77.0 | 38 |
|  |  | 5.9 | 5.72 | 2.32 | 305.7 | 50 | 52.0 |  |
| 27 | GG-PAA binder + Pressure optimized | 6.2 | 8.49 | 1.05 | 108.5 | 120 | 71.0 | 71p |
| 28 | $CsNO_3$ additive + Dopamine coating on separator | 6.74 | 9.0 | 4.2 | 355.5 | 90 | 73.3 | 28 |
|  | **This work** | 5.1 | 5.8 | 4.0 | 525.1 | 500 | 73.1 |  |
|  |  | 10.5 | 11.5 | 4.0 | 255.0 | 300 | 79.0 |  |